Binding of Chondroitin 4-Sulfate to Cathepsin S Regulates Its Enzymatic Activity

ARTICLE *in* BIOCHEMISTRY · AUGUST 2013

Impact Factor: 3.02 · DOI: 10.1021/bi400925g · Source: PubMed

BIOCHEMISTRY
including biophysical chemistry & molecular biology

Article

pubs.acs.org/biochemistry

Binding of Chondroitin 4-Sulfate to Cathepsin S Regulates Its Enzymatic Activity

Juliette Sage,[†,‡] Florian Mallèvre,[§] Fabien Barbarin-Costes,[∥] Sergey A. Samsonov,[⊥] Jan-Philip Gehrcke,[⊥] Maria Teresa Pisabarro,[⊥] Eric Perrier,[‡] Sylvianne Schnebert,[‡] André Roget,[§] Thierry Livache,[§] Carine Nizard,[‡,@] Gilles Lalmanach,[†,∥] and Fabien Lecaille*[,†,∥]

[†]INSERM, UMR 1100, Pathologies Respiratoires: protéolyse et aérosolthérapie, Centre d'Etude des Pathologies Respiratoires, Université François Rabelais, F-37032 Tours cedex, France

[‡]Louis Vuitton Moët Hennessy (LVMH-Recherche), F-45800 Saint Jean de Braye, France

[§]INAC CEA Grenoble, CREAB, UMR SPrAM 5819 (CEA, CNRS, UJF), F-38054 Grenoble Cedex 9, France

[∥]Département de Biochimie, Université François Rabelais, F-37200 Tours, France

[⊥]Structural Bioinformatics, BIOTEC Technical University of Dresden, Tatzberg 47-51, 01307 Dresden, Germany

[@]Laboratoire de Pharmacologie Cellulaire de l'Ecole Pratique des Hautes Etudes, Centre de Recherche des Cordeliers, F-75006 Paris, France

S *Supporting Information*

ABSTRACT: Human cysteine cathepsin S (catS) participates in distinct physiological and pathophysiological cellular processes and is considered as a valuable therapeutic target in autoimmune diseases, cancer, atherosclerosis, and asthma. We evaluated the capacity of negatively charged glycosaminoglycans (heparin, heparan sulfate, chondroitin 4/6-sulfates, dermatan sulfate, and hyaluronic acid) to modulate the activity of catS. Chondroitin 4-sulfate (C4-S) impaired the collagenolytic activity (type IV collagen) and inhibited the peptidase activity (Z-Phe-Arg-AMC) of catS at pH 5.5, obeying a mixed-type mechanism (estimated K_i = 16.5 ± 6 μM). Addition of NaCl restored catS activity, supporting the idea that electrostatic interactions are primarily involved. Furthermore, C4-S delayed in a dose-dependent manner the maturation of procatS at pH 4.0 by interfering with the intermolecular processing pathway. Binding of C4-S to catS was demonstrated by gel-filtration chromatography, and its affinity was measured by surface plasmon resonance (equilibrium dissociation constant K_d = 210 ± 40 nM). Moreover, C4-S induced subtle conformational changes in mature catS as observed by intrinsic fluorescence spectroscopy analysis. Molecular docking predicted three specific binding sites on catS for C4-S that are different from those found in the crystal structure of the cathepsin K−C4-S complex. Overall, these results describe a novel glycosaminoglycan-mediated mechanism of catS inhibition and suggest that C4-S may modulate the collagenase activity of catS *in vivo*.

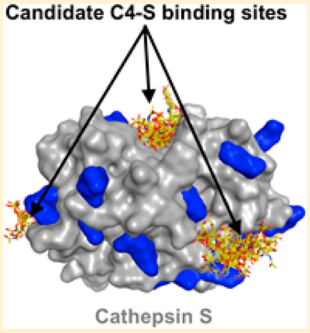

Cysteine cathepsin S (catS) is a member of the eleven-member papain-like cysteine protease family (B, C, H, F, K, L, O, S, V, W, and X). catS is a lysosomal nonglycosylated single-chain enzyme that exhibits some unique features, including the ability to remain active and stable at neutral pH. It also has a restricted expression pattern, mainly confined to antigen-presenting cells (for a review, see ref 1). catS is associated with a number of physiological processes, including MHC class II antigen presentation, and is involved in the pathogenesis of many diseases such as rheumatoid arthritis, osteoarthritis, asthma, psoriasis, and atherosclerosis, cancer, and obesity. Because of its potency in hydrolyzing various extracellular matrix (ECM) components (type IV and XVIII collagens, fibronectin, perlecan, and nidogens), intensive investigations by academic and pharmaceutical companies have focused on catS for the development of drugs that specifically target its proteolytic activity.[2]

Glycosaminoglycans (GAGs) are found on the cell surface and in ECM in most connective tissues but also in lysosomes. GAGs are linear macromolecules composed of a variable number of repeating disaccharide units and are classified into two main types: nonsulfated GAGs, including hyaluronic acid (HA), and sulfated GAGs, including chondroitin sulfate (CS) and dermatan sulfate (DS), keratan sulfate (KS), and heparin (HP) and heparan sulfate (HS). In addition to their structural role, GAGs play prominent roles in development and in many physiological processes that affect cell properties and functions.[3−5] The sulfated saccharide domains are important in providing docking sites for protein ligands, including growth factors, extracellular matrix proteins, and enzymes.[6] Chondroitin sulfate (CS) is composed of repeating disaccharide units of glucuronic acid and galactosamine, which is commonly sulfated at C-4 or C-6 of galactosamine. CS is the most

Received: July 12, 2013
Revised: August 22, 2013
Published: August 22, 2013

   dx.doi.org/10.1021/bi400925g | *Biochemistry* 2013, 52, 6487−6498

abundant GAG in human plasma (70−80% of all GAGs), with C4-S representing half of this fraction.[7] There is a growing body of evidence that GAGs may interact with various proteases, including serine proteases, matrix metalloproteases, acidic proteases, and cysteine proteases.[8−11] Indeed, low concentrations of GAGs (5−20 μg/mL) facilitate the autoprocessing of several papain-like cysteine proteases, including mammalian catB, catL, and catS[12−17] as well as trypanosomal congopain.[18] Furthermore, specific GAGs also regulate the activity of mature cathepsins B, K, and X.[19−22] As opposed to catX, HP and HS were found to increase the activity and stability of catB at neutral pH, while chondroitin 4-sulfate (C4-S) forms a stable complex with catK and enhances its collagenolytic activity.[23] The crystal and molecular structures revealed that the binding sites with C4-S are located in the R-domain of catK and are distant from its active site.[24] Conversely, high concentrations of HS and DS found in patients with mucopolysaccharidoses impair the degradation of type II collagen by catK.[25] Also, intralysosomal membrane binding GAGs, in particular CS, inhibit the activities of specific lysosomal enzymes, including the elastinolytic activities of catK and catV.[26−28] The differences in catalytic efficiency observed for several cysteine cathepsins in the presence of GAGs presumably reflect the differences in the electrostatic properties of cathepsins and in the backbone structure and sulfation pattern of GAGs.

According to the ubiquitous distribution of GAGs, the aim of this study was to examine the effect of GAGs of different structures and charges densities (HP, HS, C4-S, C6-S, DS, and HA) on the activity of catS. We report here for the first time that C4-S significantly inhibited both the collagenolytic activity (type IV collagen) and the peptidase activity (Z-Phe-Arg-AMC) of catS at acidic pH and delayed the processing of procatS, in a concentration-dependent manner. Further, interactions between C4-S and catS were analyzed by gel filtration, intrinsic fluorescence spectroscopy, surface plasmon resonance, and molecular dynamics simulations.

MATERIALS AND METHODS

Materials. Z-Phe-Arg-AMC (benzyloxycarbonyl-phenylalanyl-arginine-4-methylcoumarin) was purchased from Bachem (Bubendorf, Switzerland). Chondroitin 4-sulfate from bovine trachea (~20−30 kDa), chondroitin 6-sulfate from shark cartilage (~63 kDa), low-molecular mass heparin from porcine intestinal mucosa (15−17 kDa), heparan sulfate from bovine kidney (~14 kDa), dermatan sulfate from porcine intestinal mucosa (~13−14 kDa), and hyaluronic acid from *Streptococcus equi* (1400 kDa) were from Sigma-Aldrich (St Quentin Fallavier, France; catalog numbers C8529, C4384, H4784, H7640, C3788, and 53747, respectively). GAGs were diluted to a concentration of 30 mg/mL [i.e., 3% (w/v) stock solution] in 0.1 M sodium acetate buffer (pH 5.5) prior to further studies.

Expression and Purification of catS. The human procathepsin S clone in the pRSTEB vector was a kind gift from K. Schilling (Institute of Biochemistry I, Friedrich-Schiller-University, Jena, Germany). Procathepsin S was expressed in the form of inclusion bodies in *Escherichia coli* strain BL21(DE3)pLysS. Expression, maturation, and purification of recombinant catS were performed as described previously.[29] The active concentration was determined by titration with E-64 [L-*trans*-epoxysuccinylleucylamido(4-guanidino)butane] (Sigma-Aldrich). Unless otherwise stated, assays were conducted at 37 °C in the activity buffer of catS [0.1 M sodium acetate buffer (pH 5.5) containing 2 mM DTT and 0.01% Brij35].

Regulation of Collagen IV Proteolysis. catS (10 nM) was preincubated for 1 h with each GAG [0.15% (w/v)] in activity buffer. Type IV collagen (0.8 mg/mL, Sigma-Aldrich) was then added to the mixture and incubated for 4 h. Reduced samples were deposited via 10% sodium dodecyl sulfate−polyacrylamide gel electrophoresis (SDS−PAGE), and fragments were revealed by Coomassie blue. Densitometry analysis of the remaining α1 and α2 chains of type IV collagen was performed using ImageJ (http://imagej.nih.gov/ij/). Alternatively, the same protocol was performed at pH 7.4 [0.1 M sodium phosphate buffer (pH 7.4) containing 2 mM DTT and 0.01% Brij35].

The hydrolysis of fluorogenic DQ-collagen IV (15 μg, Molecular Probes, Life Technologies, Saint Aubin, France) was assessed in the presence of catS (2 nM) previously incubated for 1 h with each GAG (0.15%) in activity buffer. The release of fluorescence (λ_{ex} = 495 nm; λ_{em} = 515 nm) was followed in 96-well microtiter plates (Nunc) by a SpectraMax Gemini spectromicrofluorimeter (Molecular Devices, Saint Grégoire, France), and slopes were calculated with Softmaxpro (Molecular Devices). Assays were performed in triplicate and repeated two independent times. Values shown are means ± the standard deviation (SD).

Regulation of Peptidase Activity. catS (1 nM) was incubated in the presence or absence of GAG (0.15 or 0.3%) for 1 h in both activity buffers (pH 5.5 and 7.4). After the fluorogenic substrate Z-Phe-Arg-AMC (5 μM) had been added, residual activities were measured by a Gemini spectrofluorimeter (λ_{ex} = 350 nm; λ_{em} = 460 nm). Experiments were also performed in the presence of NaCl (0−1.5 M). Assays were performed in duplicate and repeated three times in separate experiments, and relative data are given as means ± SD.

Steady-state kinetics were assessed as previously described.[30] After preincubation of catS (1 nM) for 1 h in the presence or absence of GAG (0.15%) in activity buffer, the enzymatic activity was followed by monitoring the fluorescence release of Z-Phe-Arg-AMC (Kontron SFM 25 spectrofluorimeter; λ_{ex} = 350 nm; λ_{em} = 460 nm). The values of k_{cat} and K_m were determined graphically from a Hanes linear plot using various concentrations of substrate (1−100 μM), and the accuracy of K_m and k_{cat} values was confirmed by nonlinear regression analysis (substrate concentration of 1−100 μM). The second-order rate constant (k_{cat}/K_m) was measured under pseudo-first-order conditions, i.e., using a substrate concentration far below the K_m. Experiments were performed in triplicate. Kinetic data were determined using Enzfitter (Biosoft, Cambridge, U.K.) and are reported as means ± SD.

Further, the relative activity of catS was recorded by measuring the rates of Z-Phe-Arg-AMC (2.5−15 μM) substrate hydrolysis at different C4-S concentrations (0−0.3%). Data were plotted according to Hanes−Woolf plots,[31] using the equation $S/v = f(S)$. Inhibition data were fit by nonlinear regression analysis using the mixed model inhibition to determine the equilibrium dissociation constant (K_i) (GraphPad Prism). All measurements were performed three times in duplicate.

Maturation of procatS. Recombinant procathepsin S (10 μg) was incubated in 0.1 M sodium acetate buffer (pH 4.0), 2 mM DTT, 2 mM EDTA, and 0.01% Brij35 at 37 °C for up to 5 h in the absence or presence of C4-S (0.0025, 0.15, and 0.3%). Aliquots were removed at timed intervals from 1 to 300 min.

Following incubation, the samples were resuspended in SDS−PAGE loading buffer, boiled, and separated by 15% SDS−PAGE under reducing conditions. Electrophoretic gels were colored by Coomassie blue staining. Experiments were performed three independent times. Densitometry analysis of unprocessed procathepsin S was performed using ImageJ (normalized data are expressed as means ± SD). In parallel, activation progress was monitored with the fluorogenic substrate Z-Phe-Arg-AMC (10 μM, final concentration). Experimental data from time course of activity were fit using the equation $dE/dt = PE(Ek_2 + k_1)$ (eq 1), as previously described.[29] E, PE, k_1, and k_2 correspond to the enzyme, the proenzyme, and the rate constants quantifying unimolecular and bimolecular processing of procathepsin S, respectively. As reported by Turk and collaborators, such a system of differential equations has no analytical solution.[15] Therefore, considering the change in the concentration of single reactants and the sum of all the species remains constant, the kinetic parameters were evaluated by simultaneous fitting of the numerically solved system to all experimental data using simple nonlinear regression.[29] All the calculations were conducted with GraphPad Prism.

Size Exclusion Chromatography. catS (10 μg) was preincubated in the presence or absence of C4-S (0.3%) for 1 h in activity buffer. Samples were then applied to a Superdex 200 column (AKTA purifier 900 HPLC system, Amersham, GE Healthcare Bio-Sciences AB, Uppsala, Sweden), previously equilibrated in the same buffer without DTT (corresponding to elution buffer) at a flow rate of 0.5 mL/min. Protein elution was monitored at 280 nm. The calibration curve was obtained using the standard protein molecular mass markers (Amersham), ferritin (450 kDa), albumin (68 kDa), chymotrypsin (25 kDa), and cytochrome c (12.5 kDa). The catS enzymatic activity was recorded (fraction size, 0.5 mL) with Z-Phe-Arg-AMC (15 μM). In parallel, C4-S was specifically revealed using the 1,9-dimethylmethylene blue (DMB) assay (Sigma-Aldrich) according to the manufacturer's instructions. Briefly, 170 μL of the DMB solution was added to each fraction (30 μL) in a microtiter plate. The absorbance at 520 nm was then measured using a microtiter plate reader (VersaMax, Molecular Devices). In addition, collected fractions were separated via 15% SDS−PAGE under reducing conditions and transferred onto a nitrocellulose membrane for Western blotting. Immunoreactive catS was detected using a polyclonal goat anti-human cathepsin S antibody (1:1000, R&D Systems, Minneapolis, MN), as described previously.[32]

Intrinsic Fluorescence Spectroscopy. Fluorescence measurements were performed at 25 °C using a Varian Cary Eclipse spectrofluorimeter (Agilent Technologies). Emission spectra were recorded by excitation at 280 nm and collected over the range of 300−450 nm with slit widths set at 5 nm. All measurements were performed using a final catS concentration of 0.5 μM, initially prepared in activity buffer (pH 5.5) at 25 °C in 1 cm × 1 cm semi-micro quartz cuvettes. Increasing amounts of C4-S (0.03−0.3%) were added to the reaction mixture and incubated for an equilibration period of 5 min. In all experiments, the total change of reaction volume due to addition of C4-S was less than 10%. Emission spectra of the buffer in the presence or absence of C4-S were recorded separately and were subtracted from the protein emission spectra. Experiments were performed three independent times. The same experiments were performed with HP, DS, C6-S, and HS (0.3%).

Surface Plasmon Resonance Imaging (SPRi). Pyrrolylated C4-S was prepared by a two-step procedure involving the addition of adipic acid dihydrazide at the carbohydrate reducing end and then coupled to NHS-pyrrole [*N*-hydroxysuccinimidyl-6-(pyrrolyl)caproate] as described previously.[33,34] Briefly, C4-S was dissolved at a concentration of 0.15% (w/v) in 0.1 M sodium acetate buffer (pH 5.0) with 50 mM adipic acid dihydrazide and then incubated at 56 °C for 48 h. The reaction products were freeze-dried after purification in water on a PD MidiTrap G-10 column (GE Healthcare). C4-S hydrazide dissolved at 5 mM in phosphate-buffered saline was then incubated for 2 h at room temperature with NHS-pyrrole at 10 mM in DMSO in a final PBS/DMSO (v/v) buffer. The reaction products were freeze-dried after purification in water by using a PD MidiTrap G-10 column and then stored at −20 °C. Pyrrolylated C4-S was solubilized in a polymerization solution [0.1 M sodium phosphate buffer (pH 6.8) containing 10% glycerol and 20 mM pyrrole] and then immobilized on the gold surface of a precleaned SPRi biochip by the polypyrrole electrospotting process. Biochip was used in SPRi-lab apparatus (λ = 650 nm; from Horiba Scientific-GenOptics). SPRi measurements were taken in a 10 μL hexagonal flow cell connected to PEEK tubing with a degassing system (Alltech) and a syringe pump (Tecan Cavro), in sodium acetate buffer (100 mM, pH 5.5) at a rate of 50 μL/min and 25 °C. The surface was blocked with 1% BSA (Sigma-Aldrich) before injection of catS (from 50 to 400 nM). The regeneration was conducted with 1 M NaCl. All data were analyzed during the experiment with dedicated SPRi-view software (Horiba Scientific-GenOptics) and later by Origin software (OriginLab). Fits were performed following a classical Langmuir model:

$$\Delta R = (\Delta R_{max} C)/(K_d + C) \quad (2)$$

where R, C, and K_d correspond to the reflectivity, the concentration of the enzyme, and the equilibrium dissociation constant, respectively.

Molecular Docking. The X-ray structures of catS in complex with the inhibitor *N*-((2*S*)-3-methyl-2-{1-[(*E*)-2-oxohept-5-en-3-yl]-1,2,3-triazol-4-yl}butan-2-yl)benzamide [Protein Data Bank (PDB) entry 2H7J[35]], the procatS C25A mutant (PDB entry 2C0Y[36]), and catK (PDB entry 3C9E[24]) were used for calculations. The unbound structure of catS was obtained by removing the inhibitor from the complexed structure and by subsequent minimization of the binding site using the AMBER 99 force field as implemented in MOE (Molecular Operating Environment, Chemical Computing Group, Montreal, QC). The substrate Z-Phe-Arg-AMC was built in MOE and then docked to the substrate binding site of catS with Autodock using standard parameters for the Lamarckian genetic algorithm.[37] The modeled complex of catS with Z-Phe-Arg-AMC, which was found to be most similar to that of catS with the inhibitor (PDB entry 2H7J), was used as a receptor in the case of docking of C4-S and C6-S to catS with the bound substrate. The modeled complex structure was minimized in MOE, and the resulting refined model was used for docking calculations with GAGs. The structures of tetra- and hexasaccharides of C4-S and C6-S were modeled on the basis of the structure of hexameric C4-S available in the PDB (entry 1C4S, fiber diffraction[38]). Their geometries were optimized with the AMBER99 force field implemented in MOE. Blind docking of flexible tetra- and hexasaccharides of C4-S and C6-S to the surface of catK, unbound catS, and catS

dx.doi.org/10.1021/bi400925g | *Biochemistry* 2013, 52, 6487−6498

in complex with Z-Phe-Arg-AMC was conducted using Autodock. In all docking calculations, the Gasteiger charges were assigned to the protein and Z-Phe-Arg-AMC by the Autodock default procedure, while the charges for C4-S and C6-S were obtained from GLYCAM06.[39] Sulfate charges for sulfated monosaccharide units within C4-S and C6-S were obtained from the literature.[40] The atomic potential grid of the proteins was calculated with a spacing of 0.5 Å. The Lamarckian genetic algorithm was used as the search algorithm, with an initial population size of 300 and a termination condition of 10000 generations or 999500000 energy evaluations. A total of 1000 independent runs were performed. For clustering analysis, 50 and 100 top docking solutions were taken into account. Spatial clustering of the docking solutions was performed using the DBSCAN algorithm[41] with a neighborhood search radius of 4 Å. The distance between two structures was defined to be the root-mean-square deviation of atomic distances, while pairing up nearest atoms of the same type. This distance metric is invariant under symmetry transformations applied to GAGs. For further analysis, we considered only the clusters corresponding to the 50 top scoring solutions that had at least four members and the 100 top scoring solutions that had at least 10 members.

Statistical Analysis. All experiments were performed in duplicate or triplicate and repeated at least twice as independent experiments. The statistical significance was tested using the nonparametric two-way Friedman test. Data shown from Coomassie blue gel staining and Western blot analysis are from representative experiments. A P value of less than 0.01 was considered statistically significant ($P < 0.01$).

RESULTS

Type IV Collagen Proteolysis in the Presence of GAG. Type IV collagen, a major component of the basal lamina of blood vessels, is a substrate of catS.[32,42] Here, catS was incubated at pH 5.5 with type IV collagen in the presence of GAGs (HP, HS, C4-S, C6-S, DS, and HA) at a concentration of 0.15%, corresponding to physiological concentrations found in human synovial and wound fluids.[43,44] As shown in Figure 1A, C4-S and to a less extent HS strongly reduced the level of degradation of triple-helical α1(IV) and α2(IV) chains, and the effect was reversed in the presence of 0.5 M NaCl (data not shown). In contrast, the nonsulfated HA enhanced the degradation of type IV collagen by catS. Moreover, a slight increase in the level of proteolysis of type IV collagen was observed in the presence of DS. Of note, in the absence of catS, type IV collagen was sensitive to spontaneous denaturation after incubation for 4 h in the presence of 0.15% HA, but not with other sulfated GAGs (HP and C6-S) (data not shown).

The modulation of the collagenolytic activity of catS by C4-S was confirmed using as substrate, the fluorogenic DQ-collagen IV (Figure 1B). Indeed, C4-S proved to be the most effective GAG tested because it significantly reduced ($P < 0.01$) the residual activity of catS (remaining activity, 36 ± 4%). In the presence of HS, the collagenolytic activity was found to be substantially decreased as well (remaining activity, 73 ± 5%), while none of the other GAGs impaired the activity of catS. In contrast to related cysteine cathepsins, catS is stable and active at neutral pH and can be regarded as a potential participant in the proteolysis of ECM components extracellularly. Thus, in another set of experiments, we evaluated the influence of C4-S at pH 7.4. Albeit the hydrolysis of type IV collagen by catS was less efficient than at pH 5.5, a subtle reduction (10%) in the

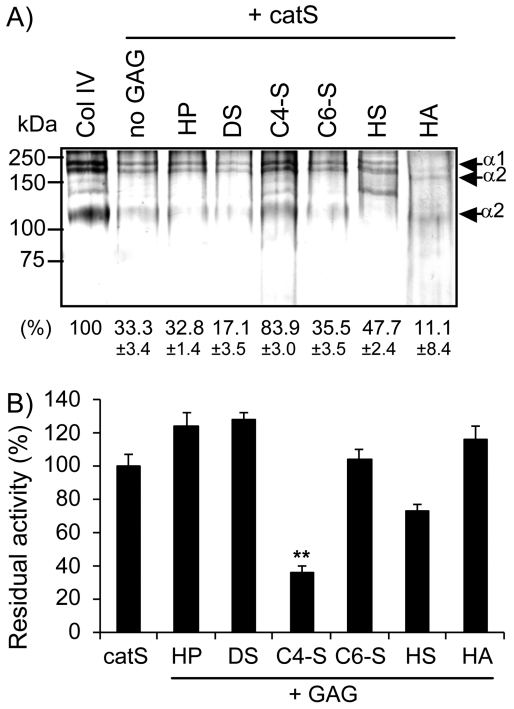

Figure 1. Effect of GAGs on the hydrolysis of type IV collagen by catS. (A) Type IV collagen (0.8 mg/mL) was incubated with catS (10 nM) in the absence or presence of 0.15% (w/v) GAGs (HP, heparin; DS, dermatan sulfate; C4-S, chondroitin 4-sulfate; C6-S, chondroitin 6-sulfate; HS, heparan sulfate; HA, hyaluronic acid). The digestion experiments were performed at 37 °C for a 4 h incubation in 0.1 M sodium acetate buffer (pH 5.5), 2 mM DTT, and 0.01% Brij35. Samples were deposited on a 10% SDS–PAGE gel, and fragments were revealed by Coomassie blue. Percentages (densitometry analysis) of residual type IV collagen are shown ± SD. (B) Similar assays were performed with the fluorogenic DQ-collagen IV substrate (15 μg) incubated for 1 h at 37 °C with catS (2 nM) in the absence or presence of 0.15% (w/v) GAGs. Experiments were performed three independent times (**$P < 0.01$ vs control).

level of degradation of both α1 and α2 chains was observed in the presence of increasing concentrations of C4-S (data not shown). Nevertheless, the different Coomassie blue-stained proteolysis products, in particular two bands (with apparent masses of 135 and 53 kDa), were weakly stained in the presence of C4-S, indicating that C4-S partly impaired the collagenase activity of catS at pH 7.4.

Effect of GAGs on the Hydrolysis of Peptidyl Z-Phe-Arg-AMC. The effect of GAGs on the peptidase activity of catS was studied by monitoring the hydrolysis of the fluorogenic dipeptidyl substrate Z-Phe-Arg-AMC (Figure 2A). As observed for type IV collagen, C4-S, HS, and to a lesser extent C6-S significantly reduced the peptidase activity of catS at pH 5.5 (i.e., 47.5 ± 1, 48.9 ± 1, and 73.8 ± 2%, respectively). Further, increasing the concentration of C4-S, HS, and C6-S (0.3%) resulted in an additional ~1.5-fold reduction in the residual activity of catS. In contrast, HP, DS, and HA had no apparent influence. The addition of NaCl restored catS activity in a dose-dependent manner (Figure 2B). However, the activity of catS was not fully recovered (70 ± 3%) when the enzyme was incubated in the presence of C4-S (0.3%) and NaCl (1.5 M). This apparent discrepancy may be explained in part by the ionic strength (I) of the buffer used. While the ionic strength of 0.1 M sodium acetate buffer (pH 5.5) is 0.087 M (theoretical value,

dx.doi.org/10.1021/bi400925g | Biochemistry 2013, 52, 6487–6498

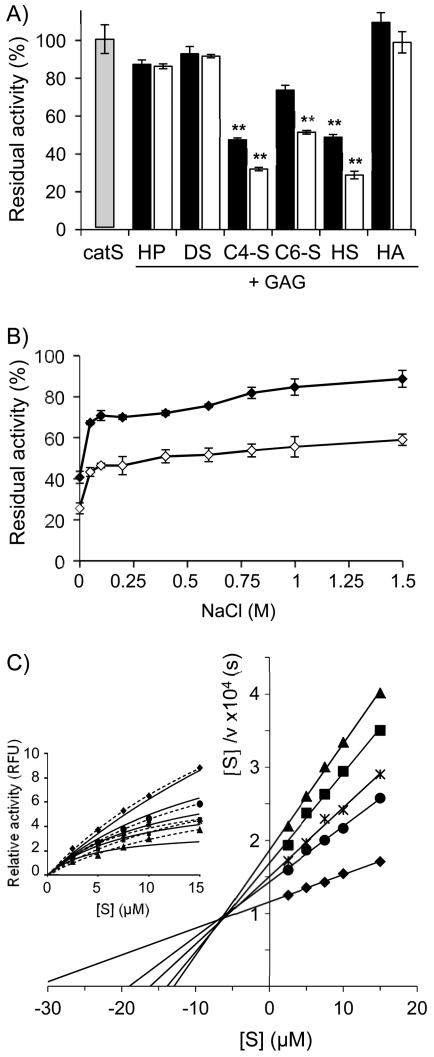

Figure 2. C4-S impairs the hydrolysis of Z-Phe-Arg-AMC. (A) catS (1 nM) was preincubated alone (gray bar) or with different GAGs (0.15%, black bar; 0.3%, white bar) in 0.1 M sodium acetate buffer (pH 5.5), 2 mM DTT, and 0.01% Brij35 for 1 h at 37 °C. Experiments were performed at least three independent times (**P < 0.01 vs control). (B) catS (1 nM) was preincubated for 1 h at 37 °C with 0.15% C4-S (◆) or 0.3% C4-S (◇) at pH 5.5 in the presence of different concentrations of NaCl (0−1.5 M). Hydrolysis of Z-Phe-Arg-AMC (5 μM) was monitored with a spectrofluorometer. (C) Hanes−Woolf plot analysis of catS velocity with varying Z-Phe-Arg-AMC (S) concentrations (2.5−15 μM) at a C4-S concentration of (◆) 0, (●) 0.05, (∗) 0.1, (■) 0.15, or (▲) 0.3%. The inset shows the same data plotted in Michaelis−Menten form (dashed line) and fit (solid line) by nonlinear regression analysis to determine K_i, using the mixed-type model inhibition (GraphPad Prism).

http://www.liv.ac.uk/buffers/buffercalc.html), ∼50% of the activity of catS was restored by addition of NaCl at a concentration as low as 0.05 M (corresponding ionic strength of 0.137 M). These results show that besides structural features of GAGs, it appeared likely that electrostatic interactions are important for interactions between negatively charged C4-S and catS. As a control, no autoproteolytic degradation of catS protein was observed in the presence of C4-S after a 4 h incubation (data not shown).

Kinetic parameters k_{cat}, K_m, and k_{cat}/K_m were determined to further evaluate the influence of C4-S on the catalytic activity of catS at pH 5.5 (Table 1). The presence of C4-S resulted in a k_{cat}/K_m value significant decreased by a factor of 4. This effect is mostly related to the decrease in k_{cat} (∼19-fold), while K_m is modified by a factor of ∼5. The presence of NaCl (1.5 M) abolished the effect promoted by C4-S (k_{cat}/K_m = 128 ± 22 mM^{-1} s^{-1}) with a k_{cat} (2.6 ± 0.4 s^{-1}) similar to that measured for the catS-catalyzed hydrolysis of Z-Phe-Arg-AMC (2.9 ± 0.5 s^{-1}). In addition, HS and C6-S promoted a ∼2-fold decrease in the second-order rate constant, associated with a large decrease in k_{cat} and to a lesser extent in K_m. In contrast, HA promoted a 1.5-fold increase in peptidase activity, similar to that observed with type IV collagen. These results indicated that the inhibition of catS by C4-S does not obey a simple competitive mechanism. We investigated the mechanism of inhibition by recording the rates of Z-Phe-Arg-AMC hydrolysis at different C4-S concentrations and plotting the data using the Hanes−Woolf representation. Results show that C4-S inhibited catS according to a mixed-type mechanism (Figure 2C). A tendency toward uncompetitive inhibition is most likely because the apparent K_m value is decreased in the presence of C4-S. This means that preferential binding of C4-S occurs with the complexed form between catS and Z-Phe-Arg-AMC. The K_i estimated by nonlinear regression analyses was calculated to be 16.5 ± 6 μM (Figure 2C, inset). The presence of sulfate groups and the degree of sulfation (0.8−0.9 sulfate group/disaccharide unit) are critical factors for the modulation of catS activity. Moreover, the spatial distribution of the sulfate group in CS is important, as supported by the differences in the kinetic values between C6-S and C4-S (Table 1). The same pattern was observed at pH 7.4 but to a lesser extent (data not shown). C4-S appeared to be the most efficient GAG for reducing the peptidase activity of catS in a dose-dependent manner, despite the specificity constant (k_{cat}/K_m = 50.6 ± 2 mM^{-1} s^{-1}) being reduced by a factor of 1.6 in the presence of 0.15% C4-S. Further, the inhibition of catS by C4-S (estimated K_i of 26.8 ± 10 μM) was less efficient than at pH 5.5. Because the isoelectric point of catS is close to neutral pH (calculated pI of 7.6) and the estimated overall charge of catS gave a rough value of 0.5 at pH 7.4 instead of 6.3 at pH 5.5 [Protein calculator software (http://www.scripps.edu)], these results support the idea that ionic interactions between negatively charged C4-S and positively charged residues located at the surface of catS are favored at acidic pH.

Effect of C4-S on procatS Maturation. In initial experiments, an optimal acidic pH [0.1 M sodium acetate buffer (pH 4.0), 2 mM DTT, 2 mM EDTA, and 0.01% Brij35] was found for the processing of procatS at 37 °C with a half-time of ∼40 min (i.e., time to achieve the 50% final activity of catS) (Figure 3A). Increasing amounts of C4-S (0.0025−0.3%) delayed the rate of proenzyme processing and in parallel increased the duration of the lag phase of full mature catS activity. A high concentration of C4-S (0.3%) resulted in an ∼4-fold increase in the half-time for complete procatS processing. In separate experiments, HP, DS, C6-S, and HS had no apparent effect on the rate of processing of procathepsin, even at the highest GAG concentration used (0.3%) (data not shown). These results suggest that C4-S specifically restricts the maturation of catS in a dose-dependent manner. The time course of autoactivation of procatS in the presence or absence of C4-S revealed a sigmoid-shaped curve (Figure 3B) indicative of a bimolecular process (intermolecular processing), as already discussed.[16,29,45] Using eq 1, experimental data from continuous monitoring of the autocatalytic processing of procatS were fit to

dx.doi.org/10.1021/bi400925g | Biochemistry 2013, 52, 6487−6498

Table 1. Kinetic Parameters for the Hydrolysis of Z-Phe-Arg-AMC by catS (pH 5.5) in the Presence and Absence of GAGs

GAG (0.15%)	degree of sulfation (no. of SO_4^{2-}/disaccharide)	disaccharide units[a]	k_{cat}/K_M (mM^{-1} s^{-1})	K_M (μM)	k_{cat} (s^{-1})
no GAG	–		93.0 ± 13	31.0 ± 2.6	2.90 ± 0.50
with 1.5 M NaCl			105.0 ± 13	19.1 ± 0.1	2.00 ± 0.25
HP	2.5	L-IdoA2S-α(1→4)-D-GlcNS6S-α(1→4)	72.6 ± 13	7.2 ± 0.8	0.53 ± 0.08
DS	1.1	L-IdoA-α(1→3)-D-GalNAc4S-β(1→4)	64.5 ± 12	7.5 ± 0.9	0.49 ± 0.11
C4-S	0.9	D-GlcA-β(1→3)-D-GalNAc4S-β(1→4)	22.5 ± 0.5	6.7 ± 1	0.15 ± 0.02
with 1.5 M NaCl			128.0 ± 22	20.3 ± 0.2	2.60 ± 0.40
C6-S	0.9	D-GlcA-β(1→3)-D-GalNAc6S-β(1→4)	43.0 ± 8	15.0 ± 1.2	0.65 ± 0.14
HS	0.8	D-GlcA-β(1→4)-D-GlcNAc-α(1→4)	38.0 ± 2	4.7 ± 1.1	0.18 ± 0.04
HA	0	D-GlcA-β(1→4)-D-GlcNAc-α(1→4)	142.0 ± 12	10.5 ± 0.7	1.50 ± 0.18

[a]Abbreviations: L-IdoA2S, iduronic acid 2-sulfate *N*-glucosamine-2,6-disulfate; GlcN, *N*-glucosamine; GalNAc, *N*-acetylgalactosamine; GlcA, glucuronic acid.

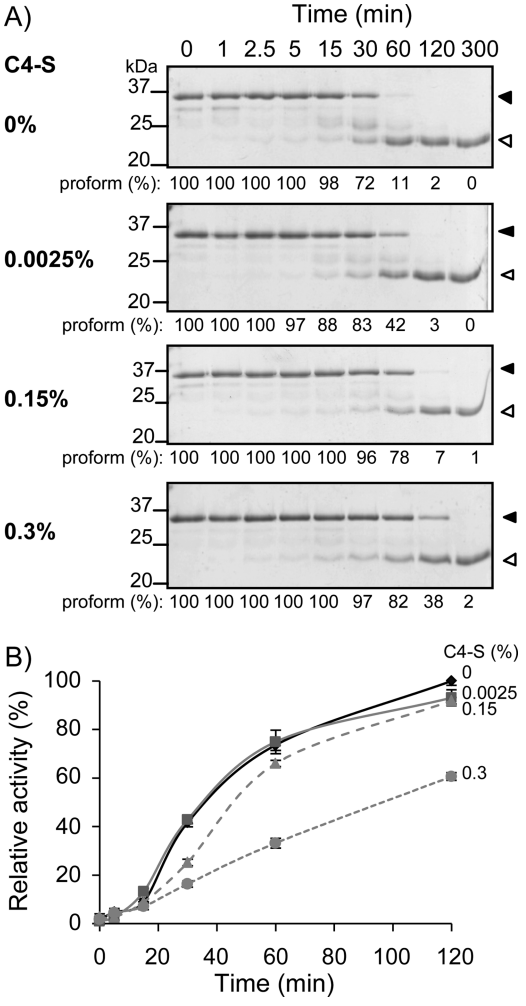

Figure 3. C4-S shifts the maturation of procatS in a dose-dependent manner. (A) SDS–PAGE analysis of procathepsin S processing in 0.1 M sodium acetate buffer (pH 4.0) containing 2 mM DTT, 2 mM EDTA, and 0.01% Brij35 at 37 °C in the presence of different concentrations of C4-S [0–0.3% (w/v)]. Samples were taken at several times during the 5 h incubation. Densitometry analyses of the remaining procatS are shown. (B) Endopeptidase activity assayed against Z-Phe-Arg-AMC (n = 3). Black arrow corresponds to procatS and white arrow to mature catS.

evaluate the effect of C4-S on the bimolecular reaction.[29] The rate of processing of procatS by fully or partially processed (active) catS is substantially decreased in the presence of increasing C4-S concentrations. Indeed, rate constant k_2 was 2.5 ± 0.4, 1.7 ± 0.4, and 0.2 ± 0.3 mM^{-1} s^{-1} for 0, 0.15, and 0.3% C4-S, respectively.

Studies of Binding of C4-S to catS. We used size exclusion chromatography to determine whether C4-S may bind tightly to catS in solution at pH 5.5 (Figure 4A). When catS was incubated with C4-S prior to being loaded on a Superdex 200 column, an additional shoulder peak was detected at 280 nm and eluted (elution volume of 10–13 mL) well ahead of the single peak detected for free catS (18–21 mL). In parallel, the enzymatic activity using Z-Phe-Arg-AMC as a subtrate was detected in both peaks (data not shown). The shoulder peak, with an apparent mass centered at 165 kDa, varied between 68 and 450 kDa, reflecting the mass heterogeneity of the commercial C4-S used, while the single peak of free catS corresponded to an apparent mass of 24 kDa. The presence of C4-S was specifically detected in 10–13 mL fractions by use of 1,9-dimethylmethylene blue (A_{520}) (see Materials and Methods). Also, in the presence of C4-S, an additional immunoreactive catS band shifted to an elution volume of 12 mL, being consistent with C4-S–catS interactions (Figure 4B). Under identical conditions, no additional peak was detected with DS.

To evaluate the binding affinity, interactions between C4-S and catS were analyzed by surface plasmon resonance (Figure 4C). After immobilization of C4-S onto a gold sensor chip, increasing concentrations of catS (from 50 to 400 nM) were passed over the surface. The results obtained (Figure 4D) showed that C4-S binds to catS with an equilibrium dissociation constant (K_d) of 210 ± 40 nM (R^2 = 0.98). Although kinetic rate constants could be determined by using a classical Langmuir equation model, the experimental values have to be regarded with care because of the mass heterogeneity that exists among commercial C4-S.

Effect of C4-S on catS Intrinsic Fluorescence Spectra. The effect of C4-S on the catS conformation was examined by intrinsic fluorescence spectroscopy, despite the fact that there are many limitations and experimental difficulties in performing topographical analysis of multi-tryptophan proteins. The fluorescence spectrum of catS that displays four tryptophan residues (Trp7, Trp26, Trp180, and Trp186) has a maximum at 334 nm (Figure 5). This is consistent with the fact that tryptophan residues are partly buried in a nonpolar environment.[46] Addition of C4-S (0.3%) resulted in an ~2-fold decrease in the fluorescence intensity at 334 nm and a slight shift of its maximum (i.e., +7 nm). This result suggests that tryptophan residues are exposed to a more hydrophilic environment, reflecting subtle structural rearrangements of catS, in the presence of C4-S. Like C4-S, both C6-S (0.3%) and

dx.doi.org/10.1021/bi400925g | *Biochemistry* 2013, 52, 6487–6498

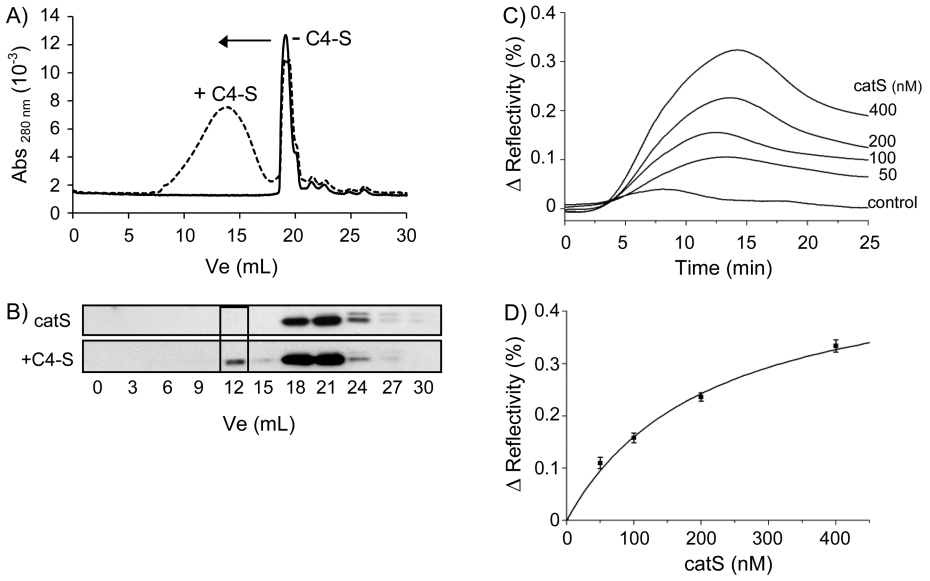

Figure 4. Interaction between C4-S and catS. Gel-filtration assay with catS (10 μg) in the presence (---) or absence (—) of C4-S (300 μg) using a Superdex 200 column. (A) Absorbance (280 nm) of eluted fractions (0.5 mL). (B) Collected fractions (0−30 mL) were transferred to the nitrocellulose membrane for catS immunodetection. The frame indicates the presence of a higher apparent molecular mass for catS. (C) catS−C4-S binding analyzed by surface plasmon resonance imaging. Compiled sensorgrams of the kinetics of the interactions between catS with C4-S-bearing biochips. In this experiment, increasing concentrations of catS (50−400 nM) were injected simultaneously onto pyrrolylated C4-S electrochemically immobilized on gold-bearing biochips. The control plot corresponds to the variation in the reflectivity from a nonfunctionalized polypyrrole spot, and Δreflectivity (%) (variation of reflectivity, expressed as a percentage of reflectivity) is the difference between the absolute reflectivity of a spot at time t and the absolute reflectivity at time zero of the same spot. (D) Fits were performed with the kinetic data according to the Langmuir model (see Materials and Methods), leading to an estimation of the catS−C4-S equilibrium dissociation constant (K_d).

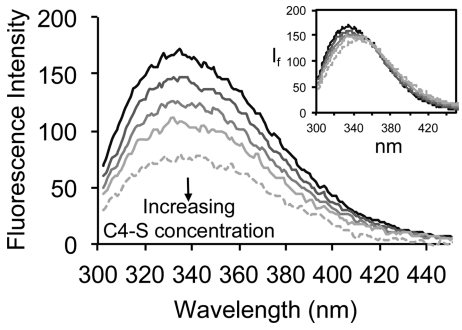

Figure 5. Intrinsic fluorescence spectra of catS in the presence of C4-S. The excitation wavelength was 280 nm, and the emission spectra were monitored from 300 to 450 nm at 25 °C. Emission fluorescence spectra of catS (500 nM) alone (black line) or in the presence of different concentrations of C4-S (gray lines for 0.03, 0.09, 0.15, and 0.3%) at pH 5.5. Spectra shown in the main panel are background-corrected fluorescence intensities (If) of catS. Emission of the buffer in the presence or absence of C4-S was recorded separately and subtracted from the catS emission spectra. The inset shows the corresponding raw spectra. Three independent experiments yielded similar results.

HS (0.3%) caused a relative Stoke shift to longer wavelengths, while no shift was observed in the presence of DS and HP.

Molecular Docking of C4-S and C6-S to catS. Our experimental data show that C4-S binds to catS and specifically modulates the activity of catS *in vitro*. To delineate the nature of the molecular mechanisms involved, and because there are currently no experimental structures available of catS complexed to C4-S, we have conducted computational studies for the identification of putative C4-S binding sites on catS. Despite the high degree of structural similarity between catS and catK (Cα atom root-mean-square deviation of 0.55 Å) and the fact that their sequences are 58 and 82% identical and similar, respectively, their electrostatic properties differ substantially (Figure 6A). Docking experiments performed with catK with C4-S identified as the most probable binding site that observed experimentally with X-rays, while no overlap of the active site and the C4-S binding site has been reported (Figure S1 of the Supporting Information). The region on catS corresponding to the GAG binding site observed in catK with X-rays (PDB entry 3C9E) is not positively charged. This means this region in catS is very unlikely to be involved in GAG binding. Indeed, docking experiments did not detect any putative C4-S binding site in this area for catS. Docking experiments performed on catS with C4-S identified three putative binding sites (Figure 6B). Site I consists of a patch formed by positively charged residues Lys39, Lys41, Lys44, Lys104, and Arg106. Site II overlaps with the substrate binding site (Figure 6C), particularly with Lys64 and Arg141, which suggests that C4-S and the substrate may sterically compete for this site. Site III is comprised of Arg120, Lys177, Arg200, and Lys202. To analyze the docking of C4-S and C6-S to catS with the bound substrate, we modeled the complex of catS with Z-Phe-Arg-AMC (see Materials and Methods). We observed that binding of C4-S to site II is favored by prior addition of the substrate Z-Phe-Arg-AMC, which is reflected by the size of the clusters resulting from the docking (Table 2; i.e., 21 cluster members vs 15 for site II and 4 members vs 11 for site I for docking with and without substrate, respectively). The binding of C4-S to site II (Figure 6C) would hinder the dissociation of Z-Phe-Arg-AMC and, therefore, may slow the reaction conducted by the protease, as we measured experimentally (Figure 2 and Table 1).

With respect to GAG length, the obtained docking scores suggested that a tetrasaccharide could be the smallest GAG unit

dx.doi.org/10.1021/bi400925g | *Biochemistry* 2013, 52, 6487−6498

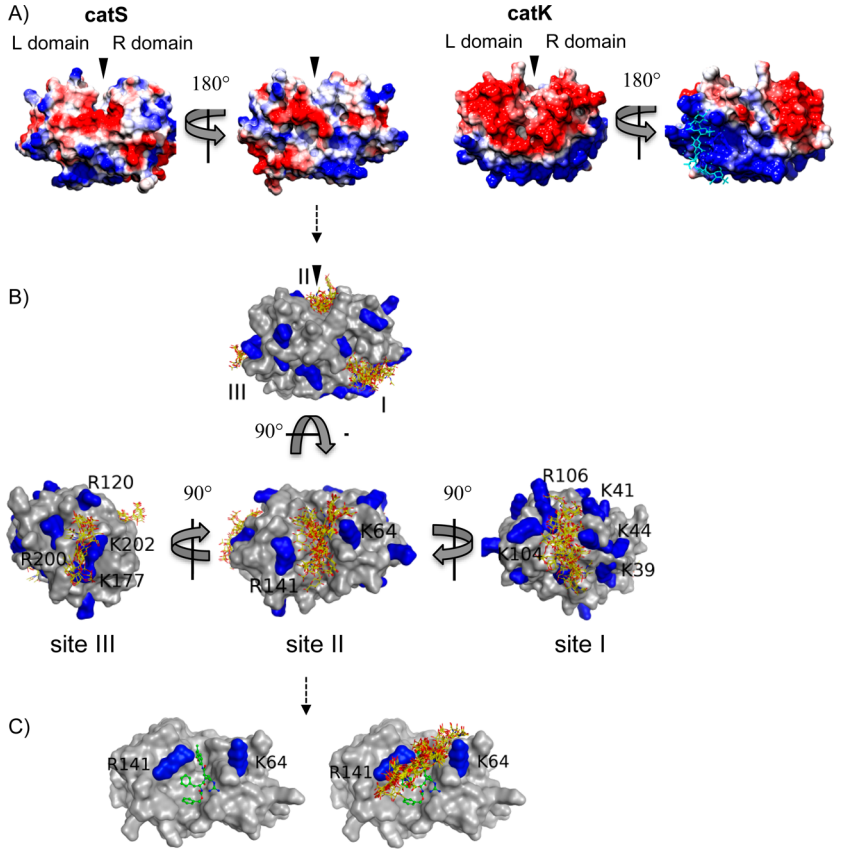

Figure 6. Structural models of binding of C4-S to catS. (A) Electrostatic potential surfaces of catS and catK. Blue areas correspond to positive charge and red areas to negative charge. A "front view" of both enzymes and a "back view" following a 180° rotation around the vertical axis are shown (left and right, respectively). The negatively charged C4-S hexasaccharide (cyan) bound to catK (back view) is shown as sticks (PDB entry 3C9E). The arrow indicates the active site of both cathepsins. (B) Back view of three putative binding sites (I–III) of C4-S on catS identified by docking. Docked C4-S molecules are shown as sticks. The surface of catS is colored gray, with Lys and Arg residues involved in recognition colored blue and labeled. C4-S binding site II is depicted below following a 90° rotation about the horizontal axis of the back view. Sites III and I on the left and right are rotated around the vertical axis by 90° relative to site II. (C) Docked Z-Phe-Arg-AMC bound to catS (left; represented as balls and sticks and as a surface, respectively). Lys and Arg residues comprising the binding site are labeled and colored blue. Docked C4-S tetrasaccharide in binding site II with Z-Phe-Arg-AMC already bound (right).

Table 2. Clustering of the Top 50 Results of 1000 Docking Runs for catS and Tetrasaccharides C4-S and C6-S

			without Z-Phe-Arg-AMC				with Z-Phe-Arg-AMC				
GAG	site	cluster size	E_{min} [a]	$\langle E\rangle$ [b] ± SD	R_{min} [c]	$\langle R\rangle$ [d]	cluster size	E_{min} [a]	$\langle E\rangle$ [b] ± SD	R_{min} [c]	$\langle R\rangle$ [d]
C4-S	I	11	−17.4	−16.1 ± 0.7	1	15.7	4	−16.4	−15.7 ± 0.7	1	11.8
	II	15	−17.2	−15.8 ± 0.6	2	19.8	21	−15.8	−15.2 ± 0.3	6	14.3
	III	4	−15.8	−15.7 ± 0.1	27	29.3	10	−16.3	−15.3 ± 0.5	2	21.0
C6-S	I	27	−17.7	−16.5 ± 0.4	5	15.7	6	−17.3	−16.1 ± 0.8	1	13.2
	II	5	−17.2	−16.5 ± 0.5	12	28.8	9	−16.5	−15.7 ± 0.5-	5	17.7
	–	4	−20.0	−18.2 ± 1.3	1	3.8					
	III	4	−17.9	−17.0 ± 0.9	3	17	8	−16.2	−15.6 ± 0.4	6	21.1

[a]Minimal energy within a cluster. [b]Mean energy within a cluster. [c]Lowest rank for all members within a cluster. [d]Difference between mean rank within a cluster and the lowest possible ranking value for this cluster size.

required for specific binding to catS, as recently observed for another GAG–protein system.[47] Upon GAG elongation, no proportional increase in docking scores was observed (Tables S1–S3 of the Supporting Information). Furthermore, comparison of docking results for C4-S and C6-S suggested a small preference of C4-S for site II and of C6-S for site I (Table 2), which corroborates the difference in K_m values measured with catS in the presence of C4-S or C6-S (Table 1).

Alternatively, we performed similar docking experiments with procatS (PDB entry 2C0Y[36]) to examine how the distribution of tetrasaccharide C4-S on the zymogen might account for the binding (Figure S2 of the Supporting Information). One binding site for C4-S was predicted on the propeptide. The C4-S binding site is located in the N-terminal part of the propeptide between helix α1 and helix α2. In particular, Lys5p, Lys17p, and Lys42p (propeptide numbering) were identified as putative residues for specific interactions. However, no C4-S binding site was observed at sites I–III obtained with the mature protein.

dx.doi.org/10.1021/bi400925g | Biochemistry 2013, 52, 6487–6498

DISCUSSION

The results of this study extend previous investigations of the regulatory effect of GAGs on cysteine cathepsins. Among tested GAGs (HP, HS, C4-S, C6-S, DS, and HA), only C4-S possesses an adapted molecular pattern that reduces significantly the level of hydrolysis by catS of type IV collagen and the dipeptidyl substrate Z-Phe-Arg-AMC. This effect relies on the catalytic machinery of catS because the Michaelis−Menten parameters for the hydrolysis of Z-Phe-Arg-AMC are altered. On the other hand, kinetic analysis revealed that the interference of catS by C4-S obeys a mixed-type inhibition approaching an uncompetitive mechanism, with an estimated K_i of 16.5 ± 6 μM. Binding of negatively charged C4-S to catS is mainly governed by ionic interactions because increasing the salt concentration restored partly its activity toward Z-Phe-Arg-AMC. The finding that HS and C6-S also influenced the endopeptidase activity of catS suggests that the degree of sulfation may be an important parameter for promoting a decrease in the type IV collagenase activity of catS, considering that HP is the most sulfated GAG with an average of ∼2.5 sulfate groups/disaccharide, DS has ∼1.1 sulfate groups/disaccharide, and C4-S, C6-S, and HS have ∼0.9 sulfate group/disaccharide. Furthermore, DS contains iduronic acid residues (instead of glucuronic acid for CS) that are proposed to exist in several conformations, thus favoring a flexibility of the oligosaccharide structure higher than the flexibility of those containing the more rigid D-glucuronic acid residues.[48] Our current observations are consistent with previous results on the potent inhibition of the collagenolytic activity of catS toward type I and II collagens by C4-S.[23] Further, we found that C4-S delayed processing of the proenzyme, particularly by interfering with the intermolecular mechanism. This result is apparently conflicting with previous reports supporting the idea that GAGs facilitate the autocatalytic processing of the proenzyme-related papain family at basic pH or acidic pH.[12−18] Nevertheless, *in vitro* studies were performed with low concentrations (5−20 μg/mL) of GAGs, while higher concentrations (>150 μg/mL) were found in human synovial and wound fluids,[43,44] which makes it difficult to compare our results with previous reports. However, it has been reported that procatS processing was impaired in the presence of a low concentration of dextran sulfate (25 μg/mL) at pH 4.[16] Moreover, higher concentrations of dextran sulfate (>100 μg/mL) resulted in a significant decrease in the level of automaturation at pH 4 of procongopain, a cathepsin L-like cysteine protease.[18] These previously published data suggest that the accelerated dissociation between the prosegment and the mature catS is favored at neutral pH, in the presence of low concentrations of C4-S (<25 μg/mL). As it has been proposed for procathepsin B,[17] it may be hypothesized that C4-S−propeptide interactions at neutral pH may induce a conformational change in procatS, which further convert the propeptide into a better substrate for catS. Our docking findings support the proposal that one site of binding to C4-S exists, located at the N-terminus of the prosegment (the putative residues for specific interactions being Lys5p, Lys17p, and Lys42p), and that interaction may occur at neutral pH. An increased concentration of GAG probably leads C4-S to compete for individual propeptide and mature catS binding. This results in an increase in the affinity for the mature enzyme compared to the propeptide that is consequently sufficient to decelerate the conversion of the proenzyme. Also, our findings show that the ability of C4-S to impair maturation of procatS at pH 4 is a specific molecular process because other sulfated GAGs, including the closely related C6-S, were not able to hinder significantly zymogen activation (data not shown). catS contains four tryptophan residues, two of which are located within the active site. Trp26 is close to Cys25 (catalytic residue), and Trp186 forms in part with His164 the bottom of the well-shaped S1′ pocket.[49] In contrast, Trp7 and Trp180 that are distant from the active site belong to the C-terminal domain composed mainly of β-strands (right domain). Despite the fact that precise topographical studies of catS are limited by the presence of four tryptophan residues, analysis of fluorescence spectra suggested that interactions between C4-S and catS led to some subtle structural rearrangement of catS.

At variance with previous studies using gel mobility shift assays, we detected the formation of a high-molecular mass complex between catS and C4-S by gel-filtration chromatography. C4-S binds to catS in the submicromolar range (K_d = 210 ± 40 nM) with an equilibrium dissociation constant lower than that of the C4-S−catK complex (K_d = 10 ± 8 nM).[24] Molecular docking identified three putative binding sites for C4-S on catS. The identified residues in catS involved in C4-S binding sites are different from those observed in the C4-S−catK crystal structure. Site I reveals a cluster of three positively charged lysine residues (Lys39, Lys41, and Lys45), opposite the substrate binding cleft of the enzyme. This motif is also found in catK but was not identified as a potential C4-S binding site. In site II, the side chains of two basic residues, Lys64 and Arg141, may interact with C4-S. The positively charged Lys64, present in the S3 subsite of catS, may provide electrostatic interactions that are unique within the cysteine cathepsin family. In contrast, catK contains an acidic residue (Asp) at this position. Another distinctive structural feature of catS is the positively charged residue Arg141, stemming from the proximal region of the S1′ subsite and pointing toward the top of the S1 subsite (Figure S3 of the Supporting Information). It has been proposed that the guanidinium group of Arg141 may be responsible for the specificity of the cleavage of the MHC class II-associated invariant chain Ii by catS.[50] Although no heparin-binding site in catS has been demonstrated, the cationic binding sequence in site III (Lys177, Arg200, and Lys202), which is solvent-exposed, is close to a site that has been proposed as a putative heparin-binding site in papain (papain sequence of Arg188, Ile189, Lys190, and Arg191).[11]

In this report, we identify putative C4-S binding sites in catS that differ from those in the C4-S−catK complex. We propose that binding of C4-S to catS, in particular at acidic pH, may represent a novel regulatory mechanism of its collagenase activity, with biological significance according to the following arguments. Despite its high stability and activity at pH 7.4, the extracellular activity of catS does not occur necessarily in a neutral pH environment as commonly described. Indeed, pericellular pH values in inflamed tissues and in the tumor microenvironment are significantly below pH 7.4. This is presumably due to the presence of different pH modulators that are responsible for local acidification (i.e., the vacualor H^+-ATPase or voltage-gated sodium channel $Na_v1.5$)[51−53] and thus favor degradation of BM components such as type IV collagen by catS. In addition, degradation of endocytosed collagen occurs within the endosomal/lysosomal compartment of various cell types, including macrophages, which are a major source of catS. Because proteoglycan and GAG turnover occurs within lysosomes,[54] it is likely that GAGs may interact with catS and regulate its activity *in vivo*. Therefore, interactions between

dx.doi.org/10.1021/bi400925g | *Biochemistry* 2013, 52, 6487−6498

catS and both C4-S and its hydrolysis products throughout the matrix and within lysosomes may also be relevant under physiological and pathophysiological conditions. Finally, the regulation of the collagenase activity of catS by C4-S may provide valuable insights for understanding the beneficial effect of C4-S in diseases such as osteoarthritis, psoriasis, or obesity, in which catS is a validated target, because of its deleterious effects.[1,55]

■ ASSOCIATED CONTENT

Supporting Information

Representation of the docking results of the C4-S hexasaccharide with catK (Figure 1), docking results for the C4-S tetrasaccharide withd procatS (PDB entry 2C0Y) (Figure 2), model of the complex of catS and Z-Phe-Arg-AMC in the presence of C4-S (Figure 3), clustering of the top 100 results of 1000 docking runs for tetrasaccharides (Table 1), clustering of the top 50 results of 1000 docking runs for hexasaccharides (Table 2), and clustering of the top 100 results of 1000 docking runs for hexasaccharides (Table 3). This material is available free of charge via the Internet at http://pubs.acs.org.

■ AUTHOR INFORMATION

Corresponding Author

*Inserm UMR 1100, Pathologies Respiratoires: protéolyse et aérosolthérapie, Equipe: Mécanismes protéolytiques dans l'inflammation, Université François Rabelais, 10 Boulevard Tonnellé, F-37032 Tours cedex, France. E-mail: fabien.lecaille@univ-tours.fr. Telephone: (+33) 247-366-047. Fax: (33) 247-366-046.

Funding

This work was financially supported in part by LVMH-Recherche (Saint Jean de Braye, France) and by institutional funding from the Institut National de la Santé et de la Recherche Médicale (INSERM). J.S. holds a doctoral fellowship from the Association Nationale de la Recherche Technique (ANRT; CIFRE Ph.D. funding). F.M., A.R., and T.L. are funded by the Agence Nationale de la Recherche (WallArrayII Project ANR-10-GENM-0010). M.T.P. and S.A.S. are funded by the German Research Council (DFG SFB-TRR67 TPA7). J.-P.G. is funded by the Studienstiftung des deutschen Volkes.

Notes

The authors declare no competing financial interest.

■ ACKNOWLEDGMENTS

We thank Dr. Bernd Wiederanders and Dr. Klaus Schilling (Institute of Biochemistry I, Friedrich-Schiller-University) for providing the cDNA clone of human procathepsin S and for their skillfull support in analyzing the autocatalytic processing of procatS. We thank the ZIH at TU Dresden for providing high-performance computational resources and Ralf Gey for technical assistance. We also thank Dr. Francis Gauthier (Inserm UMR1100, Tours, France) for his helpful comments on mixed-type inhibition kinetics. We acknowledge Dr. Reuben Ramphal (Department of Medicine, University of Florida, Gainesville, FL) for English proofreading. R. Ramphal is currently a one-year visiting scientist at INSERM UMR 1100 (Studium Chair, Région Centre, France).

■ ABBREVIATIONS

AMC, 7-amino-4-methylcoumarin; Cat, cysteine cathepsin; C4-S, chondroitin 4-sulfate; C6-S, chondroitin 6-sulfate; DS, dermatan sulfate; DTT, dithiothreitol; E-64, L-3-carboxy-*trans*-2,3-epoxypropionyl-leucylamido-(4-guanidino)butane; GAG, glycosaminoglycan; HA, hyaluronic acid; HP, heparin; HS, heparan sulfate; Z, benzyloxycarbonyl.

■ REFERENCES

(1) Small, D., Burden, R., and Scott, C. (2011) The emerging relevance of the cysteine protease cathepsin S in disease. *Clin. Rev. Bone Miner. Metab. 9*, 122−132.

(2) Turk, B. (2006) Targeting proteases: Successes, failures and future prospects. *Nat. Rev. Drug Discovery 5*, 785−799.

(3) Häcker, U., Nybakken, K., and Perrimon, N. (2005) Heparan sulphate proteoglycans: The sweet side of development. *Nat. Rev. Mol. Cell Biol. 6*, 530−541.

(4) Bishop, J. R., Schuksz, M., and Esko, J. D. (2007) Heparan sulphate proteoglycans fine-tune mammalian physiology. *Nature 446*, 1030−1037.

(5) Alexopoulou, A. N., Multhaupt, H. A. B., and Couchman, J. R. (2007) Syndecans in wound healing, inflammation and vascular biology. *Int. J. Biochem. Cell Biol. 39*, 505−528.

(6) Gandhi, N. S., and Mancera, R. L. (2008) The structure of glycosaminoglycans and their interactions with proteins. *Chem. Biol. Drug Des. 72*, 455−482.

(7) Lamari, F. N., Theocharis, A. D., Asimakopoulou, A. P., Malavaki, C. J., and Karamanos, N. K. (2006) Metabolism and biochemical/physiological roles of chondroitin sulfates: Analysis of endogenous and supplemental chondroitin sulfates in blood circulation. *Biomed. Chromatogr. 20*, 539−550.

(8) Forteza, R., Lauredo, I., Abraham, W. M., and Conner, G. E. (1999) Bronchial tissue kallikrein activity is regulated by hyaluronic acid binding. *Am. J. Respir. Cell Mol. Biol. 21*, 666−674.

(9) Isnard, N., Robert, L., and Renard, G. (2003) Effect of sulfated GAGs on the expression and activation of MMP-2 and MMP-9 in corneal and dermal explant cultures. *Cell Biol. Int. 27*, 779−784.

(10) Beckman, M., Freeman, C., Parish, C. R., and Small, D. H. (2009) Activation of cathepsin D by glycosaminoglycans. *FEBS J. 276*, 7343−7352.

(11) Almeida, P. C., Nantes, I. L., Rizzi, C. C., Júdice, W. A., Chagas, J. R., Juliano, L., Nader, H. B., and Tersariol, I. L. (1999) Cysteine proteinase activity regulation. A possible role of heparin and heparin-like glycosaminoglycans. *J. Biol. Chem. 274*, 30433−30438.

(12) Mason, R. W., and Massey, S. D. (1992) Surface activation of pro-cathepsin L. *Biochem. Biophys. Res. Commun. 189*, 1659−1666.

(13) Ishidoh, K., and Kominami, E. (1994) Multi-step processing of procathepsin L in vitro. *FEBS Lett. 352*, 281−284.

(14) Kopitar, G., Dolinar, M., Strukelj, B., Pungercar, J., and Turk, V. (1996) Folding and activation of human procathepsin S from inclusion bodies produced in *Escherichia coli*. *Eur. J. Biochem. 236*, 558−562.

(15) Rozman, J., Stojan, J., Kuhelj, R., Turk, V., and Turk, B. (1999) Autocatalytic processing of recombinant human procathepsin B is a bimolecular process. *FEBS Lett. 459*, 358−362.

(16) Vasiljeva, O., Dolinar, M., Pungercar, J. R., Turk, V., and Turk, B. (2005) Recombinant human procathepsin S is capable of autocatalytic processing at neutral pH in the presence of glycosaminoglycans. *FEBS Lett. 579*, 1285−1290.

(17) Caglic, D., Pungercar, J. R., Pejler, G., Turk, V., and Turk, B. (2007) Glycosaminoglycans facilitate procathepsin B activation through disruption of propeptide-mature enzyme interactions. *J. Biol. Chem. 282*, 33076−33085.

(18) Serveau, C., Boulangé, A., Lecaille, F., Gauthier, F., Authié, E., and Lalmanach, G. (2003) Procongopain from *Trypanosoma congolense* is processed at basic pH: An unusual feature among cathepsin L-like cysteine proteases. *Biol. Chem. 384*, 921−927.

(19) Almeida, P. C., Nantes, I. L., Chagas, J. R., Rizzi, C. C., Faljoni-Alario, A., Carmona, E., Juliano, L., Nader, H. B., and Tersariol, I. L. (2001) Cathepsin B activity regulation. Heparin-like glycosaminoglycans protect human cathepsin B from alkaline pH-induced inactivation. *J. Biol. Chem. 276*, 944−951.

(20) Li, Z., Hou, W.-S., Escalante-Torres, C. R., Gelb, B. D., and Brömme, D. (2002) Collagenase activity of cathepsin K depends on complex formation with chondroitin sulfate. *J. Biol. Chem. 277*, 28669−28676.
(21) Novinec, M., Kovacic, L., Lenarcic, B., and Baici, A. (2010) Conformational flexibility and allosteric regulation of cathepsin K. *Biochem. J. 429*, 379−389.
(22) Nascimento, F. D., Rizzi, C. C. A., Nantes, I. L., Stefe, I., Turk, B., Carmona, A. K., Nader, H. B., Juliano, L., and Tersariol, I. L. S. (2005) Cathepsin X binds to cell surface heparan sulfate proteoglycans. *Arch. Biochem. Biophys. 436*, 323−332.
(23) Li, Z., Yasuda, Y., Li, W., Bogyo, M., Katz, N., Gordon, R. E., Fields, G. B., and Brömme, D. (2004) Regulation of collagenase activities of human cathepsins by glycosaminoglycans. *J. Biol. Chem. 279*, 5470−5479.
(24) Li, Z., Kienetz, M., Cherney, M. M., James, M. N. G., and Brömme, D. (2008) The crystal and molecular structures of a cathepsin K:chondroitin sulfate complex. *J. Mol. Biol. 383*, 78−91.
(25) Wilson, S., Hashamiyan, S., Clarke, L., Saftig, P., Mort, J., Dejica, V. M., and Brömme, D. (2009) Glycosaminoglycan-mediated loss of cathepsin K collagenolytic activity in MPS I contributes to osteoclast and growth plate abnormalities. *Am. J. Pathol. 175*, 2053−2062.
(26) Avila, J. L., and Convit, J. (1975) Inhibition of leucocytic lysosomal enzymes by glycosaminoglycans in vitro. *Biochem. J. 152*, 57−64.
(27) Avila, J. L. (1978) The influence of the type of sulphate bond and degree of sulphation of glycosaminoglycans on their interaction with lysosomal enzymes. *Biochem. J. 171*, 489−491.
(28) Yasuda, Y., Li, Z., Greenbaum, D., Bogyo, M., Weber, E., and Brömme, D. (2004) Cathepsin V, a novel and potent elastolytic activity expressed in activated macrophages. *J. Biol. Chem. 279*, 36761−36770.
(29) Kramer, G., Paul, A., Kreusch, A., Schüler, S., Wiederanders, B., and Schilling, K. (2007) Optimized folding and activation of recombinant procathepsin L and S produced in *Escherichia coli*. *Protein Expression Purif. 54*, 147−156.
(30) Lecaille, F., Chowdhury, S., Purisima, E., Brömme, D., and Lalmanach, G. (2007) The S2 subsites of cathepsins K and L and their contribution to collagen degradation. *Protein Sci. 16*, 662−670.
(31) Segel, I. (1975) *Enzyme Kinetics: Behavior and Analysis of Rapid Equilibrium and Steady State Enzyme Systems*, p 1127, John Wiley & Sons, New York.
(32) Sage, J., Leblanc-Noblesse, E., Nizard, C., Sasaki, T., Schnebert, S., Perrier, E., Kurfurst, R., Brömme, D., Lalmanach, G., and Lecaille, F. (2012) Cleavage of nidogen-1 by cathepsin S impairs its binding to basement membrane partners. *PLoS One 7*, e43494.
(33) Mercey, E., Grosjean, L., Roget, A., and Livache, T. (2007) Surface plasmon resonance imaging on polypyrrole protein chips: Application to streptavidin immobilization and immunodetection. *Methods Mol. Biol. 385*, 159−175.
(34) Bartoli, J., Roget, A., and Livache, T. (2012) Polypyrrole-oligosaccharide microarray for the measurement of biomolecular interactions by surface plasmon resonance imaging. *Methods Mol. Biol. 808*, 69−86.
(35) Patterson, A. W., Wood, W. J. L., Hornsby, M., Lesley, S., Spraggon, G., and Ellman, J. A. (2006) Identification of selective, nonpeptidic nitrile inhibitors of cathepsin S using the substrate activity screening method. *J. Med. Chem. 49*, 6298−6307.
(36) Kaulmann, G., Palm, G. J., Schilling, K., Hilgenfeld, R., and Wiederanders, B. (2006) The crystal structure of a Cys25 → Ala mutant of human procathepsin S elucidates enzyme-prosequence interactions. *Protein Sci. 15*, 2619−2629.
(37) Morris, G. M., Goodsell, D. S., Halliday, R. S., Huey, R., Hart, W. E., Belew, R. K., and Olson, A. J. (1998) Automated docking using a Lamarckian genetic algorithm and an empirical binding free energy function. *J. Comput. Chem. 19*, 1639−1662.
(38) Winter, W. T., Arnott, S., Isaac, D. H., and Atkins, E. D. (1978) Chondroitin 4-sulfate: The structure of a sulfated glycosaminoglycan. *J. Mol. Biol. 125*, 1−19.
(39) Kirschner, K. N., Yongye, A. B., Tschampel, S. M., González-Outeiriño, J., Daniels, C. R., Foley, B. L., and Woods, R. J. (2008) GLYCAM06: A generalizable biomolecular force field. Carbohydrates. *J. Comput. Chem. 29*, 622−655.
(40) Huige, C. J. M., and Altona, C. (1995) Force field parameters for sulfates and sulfamates based on ab initio calculations: Extensions of AMBER and CHARMm fields. *J. Comput. Chem. 16*, 56−79.
(41) Ester, M., Kriegel, H.-P., Sander, J., and Xu, X. (1996) A density-based algorithm for discovering clusters in large spatial databases with noise. *Proceedings of 2nd International Conference on Knowledge Discovery and Data Mining (KDD-96)*, pp 226−231, AAAI Press, Palo Alto, CA.
(42) Wang, B., Sun, J., Kitamoto, S., Yang, M., Grubb, A., Chapman, H. A., Kalluri, R., and Shi, G.-P. (2006) Cathepsin S controls angiogenesis and tumor growth via matrix-derived angiogenic factors. *J. Biol. Chem. 281*, 6020−6029.
(43) Møller, H. J., Larsen, F. S., Ingemann-Hansen, T., and Poulsen, J. H. (1994) ELISA for the core protein of the cartilage large aggregating proteoglycan, aggrecan: Comparison with the concentrations of immunogenic keratan sulphate in synovial fluid, serum and urine. *Clin. Chim. Acta 225*, 43−55.
(44) Penc, S. F., Pomahac, B., Winkler, T., Dorschner, R. A., Eriksson, E., Herndon, M., and Gallo, R. L. (1998) Dermatan sulfate released after injury is a potent promoter of fibroblast growth factor-2 function. *J. Biol. Chem. 273*, 28116−28121.
(45) Quraishi, O., and Storer, A. C. (2001) Identification of internal autoproteolytic cleavage sites within the prosegments of recombinant procathepsin B and procathepsin S. Contribution of a plausible unimolecular autoproteolytic event for the processing of zymogens belonging to the papain family. *J. Biol. Chem. 276*, 8118−8124.
(46) Eftink, M. R., and Ghiron, C. A. (1976) Exposure of tryptophanyl residues in proteins. Quantitative determination by fluorescence quenching studies. *Biochemistry 15*, 672−680.
(47) Pichert, A., Samsonov, S. A., Theisgen, S., Thomas, L., Baumann, L., Schiller, J., Beck-Sickinger, A. G., Huster, D., and Pisabarro, M. T. (2012) Characterization of the interaction of interleukin-8 with hyaluronan, chondroitin sulfate, dermatan sulfate and their sulfated derivatives by spectroscopy and molecular modeling. *Glycobiology 22*, 134−145.
(48) Casu, B., Petitou, M., Provasoli, M., and Sinaÿ, P. (1988) Conformational flexibility: A new concept for explaining binding and biological properties of iduronic acid-containing glycosaminoglycans. *Trends Biochem. Sci. 13*, 221−225.
(49) Pauly, T. A., Sulea, T., Ammirati, M., Sivaraman, J., Danley, D. E., Griffor, M. C., Kamath, A. V., Wang, I.-K., Laird, E. R., Seddon, A. P., Ménard, R., Cygler, M., and Rath, V. L. (2003) Specificity determinants of human cathepsin S revealed by crystal structures of complexes. *Biochemistry 42*, 3203−3213.
(50) Guncar, G., Pungercic, G., Klemencic, I., Turk, V., and Turk, D. (1999) Crystal structure of MHC class II-associated p41 Ii fragment bound to cathepsin L reveals the structural basis for differentiation between cathepsins L and S. *EMBO J. 18*, 793−803.
(51) Reddy, V. Y., Zhang, Q. Y., and Weiss, S. J. (1995) Pericellular mobilization of the tissue-destructive cysteine proteinases, cathepsins B, L, and S, by human monocyte-derived macrophages. *Proc. Natl. Acad. Sci. U.S.A. 92*, 3849−3853.
(52) Punturieri, A., Filippov, S., Allen, E., Caras, I., Murray, R., Reddy, V., and Weiss, S. J. (2000) Regulation of elastinolytic cysteine proteinase activity in normal and cathepsin K-deficient human macrophages. *J. Exp. Med. 192*, 789−799.
(53) Gillet, L., Roger, S., Besson, P., Lecaille, F., Gore, J., Bougnoux, P., Lalmanach, G., and Le Guennec, J.-Y. (2009) Voltage-gated Sodium Channel Activity Promotes Cysteine Cathepsin-dependent Invasiveness and Colony Growth of Human Cancer Cells. *J. Biol. Chem. 284*, 8680−8691.
(54) Winchester, B. G. (1996) Lysosomal metabolism of glycoconjugates. *Subcell. Biochem. 27*, 191−238.

(55) Palermo, C., and Joyce, J. A. (2008) Cysteine cathepsin proteases as pharmacological targets in cancer. *Trends Pharmacol. Sci. 29*, 22−28.

■ NOTE ADDED AFTER ASAP PUBLICATION

This paper was published to the Web with an error in the Figure 3 caption on September 4, 2013. This was fixed in the version published to the Web on September 9, 2013.